

STATUS OF THE GDH EXPERIMENT ON THE DEUTERON AT MAMI

O. JAHN

on behalf of the A2 and GDH Collaborations

*Institut für Kernphysik
J.-J.-Becher Weg 45
55099 Mainz, Germany
E-mail: jahn@kph.uni-mainz.de*

The GDH sum rule connects ground state properties of the nucleon with helicity dependent cross sections. To investigate these cross sections on the deuteron, experiments have been carried out in the A2-Collaboration at the Mainz Microtron, Germany, in 1998 and in 2003, using circularly polarized photons on a polarized d-butanol target. A status report of the data analysis and latest results from the pilot experiment of 1998 are given.

1. Introduction

The Gerasimov-Drell-Hearn sum rule for real photons and any compound system with spin S reads

$$\int_0^{\infty} \frac{\sigma_p(\omega) - \sigma_a(\omega)}{\omega} d\omega = \frac{4\pi^2 e^2}{m^2} \kappa^2 S, \quad (1)$$

connecting the ground state properties mass, m , and anomalous magnetic moment, κ , of the given system with the difference of the total photo-absorption cross sections for parallel ($\sigma_p(\omega)$) and antiparallel ($\sigma_a(\omega)$) alignment of the photon helicity and the system's spin. This relation is derived using very basic ingredients e.g. Lorentz and gauge invariance, unitarity, causality, and no-subtraction hypothesis, see Ref. [11]. Table 1 shows values for the right-hand side of the GDH sum rule for the lightest nuclei and the neutron as well as their anomalous magnetic moments.

For the proton, the GDH sum rule seems to be experimentally confirmed, see Ref. [12], but the situation is still not clear for the neutron. Since no free neutron target is available, one has to use bound neutron targets (e.g., the deuteron) and theoretical models to extract the neutron

Table 1. Anomalous magnetic moment and right-hand side value for the GDH sum rule for some light nuclei.

	κ	$I_{\text{GDH}}[\mu\text{b}]$
Proton	1.79	204
Neutron	-1.91	233
Deuteron	-0.14	0.65
Helium3	-8.38	497

Table 2. Comparison of contributions to the GDH sum rule for the neutron from the MAID model, see Ref. [15], with right-hand side of Equation 1.

Channel	GDH [μb]
π^0	154
π^\pm	-30
η	-10
$\pi\pi$	16 ± 10
K	2
Bianchi et al.	35 ± 11
Total	167
Right-hand side	233

contributions from the data given by experiment. In the case of a deuteron target, a simple approach would be to think of the deuteron as the sum of proton and neutron plus some nuclear binding effects, so the GDH integral could be written as

$$I_{\text{GDH}}^d = I_{\text{GDH}}^{\text{proton}} + I_{\text{GDH}}^{\text{neutron}} + I_{\text{GDH}}^{\text{nuclear effects}}. \quad (2)$$

When trying to evaluate the addends of the above equation using model predictions for all possible partial channels (e.g. predictions by MAID [15]) one ends up with quite a considerable discrepancy to the right-hand side of the GDH sum rule as is shown in Table 2. These calculations cover photon energies from the respective threshold up to 1.66 GeV. Contributions above these energies were estimated to be about $30 \mu\text{b}$ using calculations by Bianchi et al., given in Ref. [5]. Although the gap could be decreased by more recent calculations, the very existence of a discrepancy clearly shows the necessity to improve the theoretical understanding of the different reaction channels on the neutron.

An experimental test of the GDH sum rule requires doubly polarized experiments covering a very wide (theoretically infinite) energy range. Between 1998 and 2003, such experiments were carried out at the Mainz Microtron (MAMI) in Mainz, and the Electron Stretcher Accelerator (ELSA) in Bonn. The experiments covered an energy range from pion production threshold to 800 MeV at Mainz, and from 700 to 2950 MeV at Bonn. This report will focus on the pilot experiment carried out in 1998 at MAMI on a polarized d-butanol target ($\text{C}_4\text{H}_9\text{OH}$ where all hydrogen atoms (H) were replaced with deuterium (^2H)).

2. Experimental Setup at MAMI

The measurement of helicity-dependent cross sections requires circularly polarized photons, a longitudinally polarized deuteron-like target (in our case deuterated butanol), and a detector system with large momentum and angular acceptance.

A description of the experimental setup can be found in Ref. [1] and the references therein. The main detector system DAPHNE (the acronym stands for “Détecteur à grande Acceptance pour la PHysique photoNucléaire Expérimentale”) is described in detail in Ref. [3].

Circularly polarized photons were produced by the tagged photon facility (Ref. [2]) via the Bremsstrahlung process with longitudinally polarized electrons (Ref. [4]). The electron polarization was monitored on-line with a Møller polarimeter and an average value of approx. 75% was found. The helicity transfer from electrons to photons can be calculated following Ref. [16].

Longitudinally polarized deuterons were provided by a frozen-spin deuterated butanol target (Ref. [6]). The average target polarization for the 1998 pilot runs was approx. 30%.

3. Data Analysis and Results

3.1. Total Cross Section

Only data recorded by DAPHNE will be presented here. An inclusive method was used to extract the total photo-absorption cross sections σ_p and σ_a . This method has already been applied to data from the proton, both unpolarized and polarized (Ref. [13]), and to unpolarized deuterium data as well (Ref. [14]).

Since DAPHNE was optimized to detect charged particles, about 75% of the total photo-absorption cross section is accessible by the detection of events with charged hadrons in the final state. Approximately 15–20% of the total cross section can be found using events with one π^0 in the final state but no accompanying charged particle detected (N_{π^0}). The efficiency of DAPHNE for detecting π^0 final states (ε_{π^0}) was determined via a GEANT simulation. ε_{π^0} is non-zero for all angles and energies, hence no extrapolation is necessary in this case. Only corrections ($\approx 5\%$) for charged pions emitted into angular and momentum regions outside DAPHNE’s acceptance ($\Delta N(\pi^\pm)$) are needed.

Using above notation, the total photo-absorption cross section can be

written as

$$\sigma_{\text{tot}} \propto N_{\text{Hadrons}} = N_{\text{ch}} + N_{\pi^0} \varepsilon_{\pi^0}^{-1} + \Delta N(\pi^\pm). \quad (3)$$

Figure 1 shows preliminary results on the unpolarized deuteron as well as results of a former measurement also using DAPHNE (Ref. [14]). The good agreement indicates that the detector is well understood and the analysis method can be applied to polarized data.

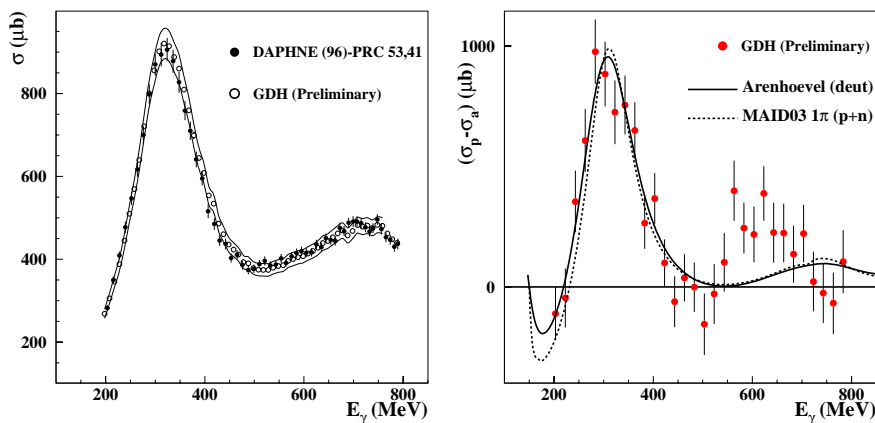


Figure 1. Energy dependence of the polarized total photo-absorption cross section σ_{tot} on the deuteron. Open circles: preliminary 1998 data (Ref. [17]); filled circles: former measurement also using DAPHNE detector (Ref. [14]). The systematic error is represented by the error band.

Figure 2. Preliminary results for the difference of the total photo-absorption cross sections for the two relative spin configurations σ_p and σ_a between 200 and 800 MeV photon energy. Only the 1998 pilot experiment data and their statistical errors are shown.

Results for the total cross section difference ($\sigma_p - \sigma_a$) are shown in Figure 2 (Ref. [17]), confronted with calculations by Arenhövel's group (Ref. [19–21], solid curve) and a MAID 2003 calculation (dotted curve) that just sums contributions for the free proton and the free neutron. Both curves only include single pion channels. The differences between the two model predictions and the data are seen much more clearly in Figure 3 which depicts the GDH integral function, also known as running GDH integral,

$$I_{\text{GDH}}(E_\gamma) = \int_{200 \text{ MeV}}^{E_\gamma} \frac{\sigma_p(\omega) - \sigma_a(\omega)}{\omega} d\omega \quad (4)$$

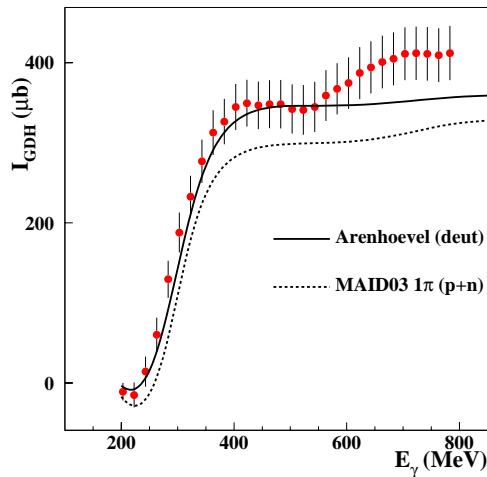


Figure 3. Running GDH integral for the deuteron showing preliminary results. For details see text.

in units of μb . The Arenhövel calculation agrees with the data very well in the Δ region, while it is clear that MAID fails because binding effects, deuteron disintegration, coherent π^0 production and final state interactions are not taken into account. Not all corrections have yet been applied to the data above double pion production threshold, so changes on the order of at most 10% are still to be expected.

3.2. Photodisintegration

The analysis for photodisintegration below $E_\gamma = 450$ MeV is quite straightforward. Only events with one charged track in DAPHNE are taken into account. Particle identification is achieved using an extended $\Delta E/E$ -method, named “range fit,” given in Ref. [7], and kinematics of this two-body process allows for separation from competing reactions. Corrections for detection efficiency and for solid angle due to the finite target length were determined with GEANT simulations. Again, this analysis was first applied to unpolarized deuterium data giving results that nicely agree with data from Ref. [9].

Above $E_\gamma = 450$ MeV a considerable fraction of the protons from photodisintegration have enough kinetic energy to pass through DAPHNE and hence cannot be distinguished from pions originating from the reactions $\vec{\gamma} + \vec{d} \rightarrow N + N + \pi^\pm$. In addition, most of the single charged parti-

cle events in this energy region are due to pion photoproduction channels while protons from photodisintegration are only a small fraction of the total number of events. Due to these complications, the separation of the photodisintegration channel needs a more sophisticated analysis procedure that has not yet been applied. Therefore, only data for photon energies below 450 MeV will be presented here.

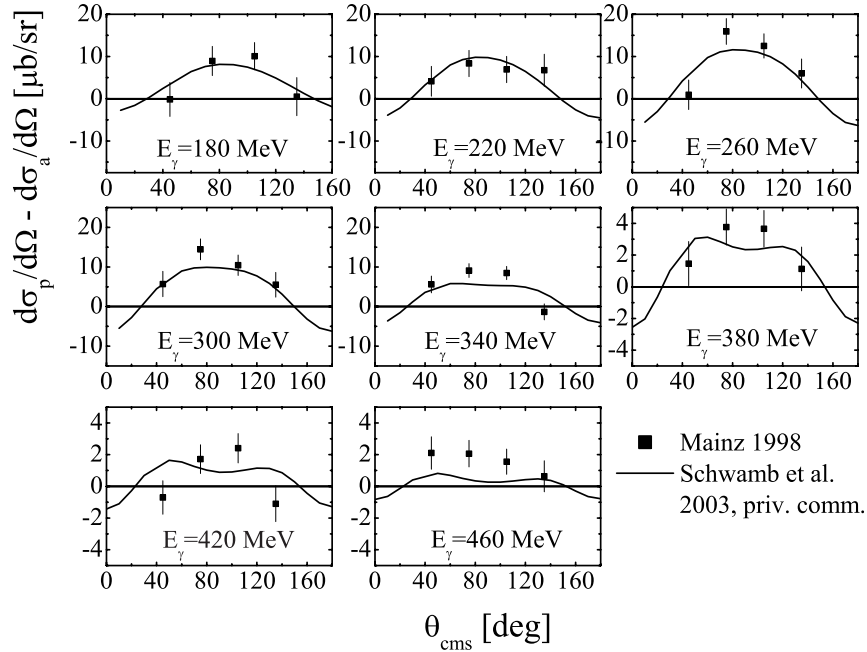


Figure 4. Preliminary results for the dependence of the difference of differential photodisintegration cross sections on the polar angle θ of the proton for several photon energies E_γ between 180 and 460 MeV. θ is given for the centre-of-mass system in degrees. Only statistical errors are shown. The line shows calculations by Schwamb et al. (Refs. [19]–[22]).

Preliminary results for differential photodisintegration cross sections for several photon energies are shown in Figure 4. Also shown are calculations by Schwamb et al. (Refs. [19–22]). Since both agree, the calculations were used for the determination of the difference of the total photodisintegration cross sections to extrapolate to full solid angle coverage. The results are presented in Figure 5 compared to the calculations by Schwamb. The systematic error has not yet been considered but is expected to be below 10%.

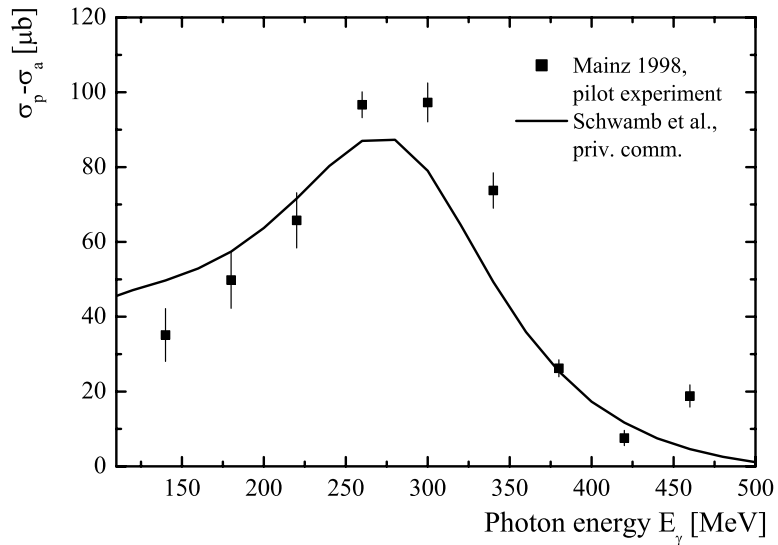


Figure 5. Preliminary results for the energy dependence of the difference of the total photodisintegration cross sections σ_p and σ_a between 140 and 460 MeV photon energy. Only statistical errors are shown. The line represents calculations by Schwamb et al., see Refs. [19]–[22].

3.3. Single Pion Production

Only the partial channels

$$\vec{\gamma} + \vec{d} \longrightarrow p_s + p + \pi^- \quad (5)$$

and

$$\vec{\gamma} + \vec{d} \longrightarrow n_s + p + \pi^0 \quad (6)$$

have been taken care of as of yet. The index “s” denotes the nucleon being a spectator, i.e. the incoming photon interacts only with one nucleon in the deuteron while the second nucleon is emitted with its Fermi momentum. The spectator will not leave the target material which means it will not be detected. Hence, there is not enough information available to reconstruct the full kinematics of an event, i.e. only angles in the lab frame can be specified.

Reaction 5 can be uniquely accessed below $E_\gamma = 450$ MeV by selecting two charged tracks in DAPHNE, since all other possible partial channels

result in at most one charged track in DAPHNE. Above $E_\gamma = 450$ MeV, one has to apply additional missing mass cuts to separate from $\vec{\gamma} + \vec{d} \rightarrow p_s + p + \pi^- + \pi^0$.

The only way to access Reaction 6 is the detection and identification of the proton in the final state. This means that no reconstruction of the full kinematics on an event by event basis is possible. Again, one has to apply missing mass cuts to separate this reaction from photodisintegration which is the competing reaction.

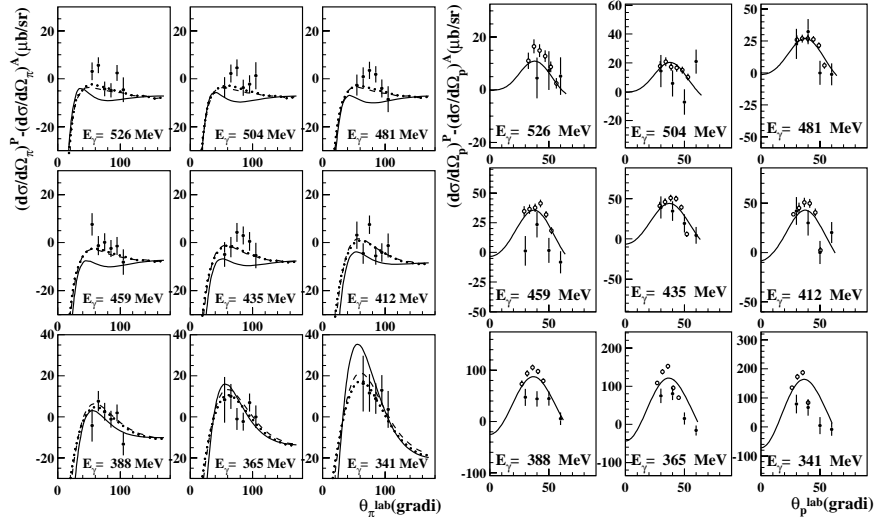


Figure 6. Difference of the differential cross sections versus θ of the pion in the *laboratory system* for the reaction $\vec{\gamma} + \vec{d} \rightarrow p_s + p + \pi^-$. The figure was taken from [18]. For details see text.

Figure 7. Difference of the differential cross sections versus θ of the proton in the *laboratory system* for the reaction $\vec{\gamma} + \vec{d} \rightarrow n_s + p + \pi^0$ (solid circles). For comparison, also data of π^0 production on the free proton are shown (open circles). The figure was taken from [18]. For details see text.

Figure 6 depicts preliminary results for the difference of the differential cross sections $(d\sigma/d\Omega)_p - (d\sigma/d\Omega)_a$ versus θ of the pion in lab frame for the reaction $\vec{\gamma} + \vec{d} \rightarrow p_s + p + \pi^-$. The curves show several Arenhövel calculations (Ref. [10]): the solid curve gives the contribution of π^- production on the free neutron, the dashed curve is the reaction on the deuteron in impulse approximation, while the dotted curve includes both impulse approximation

and final state interactions.

Figure 7 presents preliminary results for the difference of the differential cross sections $(d\sigma/d\Omega)_p - (d\sigma/d\Omega)_a$ for the reaction $\vec{\gamma} + \vec{d} \rightarrow n_s + p + \pi^0$ plotted versus the polar angle θ of the proton, again in lab frame (solid circles). Also shown are data on the free proton (open circles) and a corresponding MAID calculation. The energy evolution of the discrepancy between free proton and deuteron data allows one to study the energy dependence of the binding effects in the deuteron.

4. Outlook

There are several projects which will be realized in the near future that will allow improvement of the existing data base on the deuteron:

- The Mainz Microtron is being upgraded at this time to a maximum electron beam energy of 1.5 GeV (MAMI C).
- The tagged photon facility will also be upgraded to the electron beam energy of 1.5 GeV.
- The Crystal Ball detector will be available to measure neutral reaction channels that were not accessible to the DAPHNE detector.
- The A2 collaboration is in the process of building a polarized target of its own.

With these changes, it will be possible to investigate all partial reaction channels between pion threshold and ≈ 1.4 GeV photon energy at high detection efficiency and with a solid angle coverage of almost 100%.

References

1. J. Ahrens et al., *Phys. Rev. Lett.* **87** 2 (2001).
2. I. Anthony et al., *NIM* **A301** 230 (1991); S.J. Hall et al., *NIM* **A368** 698 (1996).
3. G. Audit et al., *NIM* **A301** (1991) 473–481.
4. K. Aulenbacher, *NIM* **A391** 498 (1997).
5. N. Bianchi and E. Thomas, *Phys. Lett.* **B450** (1999) 439.
6. C. Bradtke et al., *NIM* **A436** 430 (1999); C. Bradtke, Ph.D. thesis, University of Bonn, 2000.
7. A. Braghieri et al., *NIM* **A343** (1994) 623–628.
8. R. Crawford, Ph.D. thesis, University of Glasgow, 1994.
9. R. Crawford et al., *Nucl. Phys.* **A603** (1996) 303.
10. E.M. Darwish, Ph.D. thesis, University of Mainz, 2002.
11. S.B. Gerasimov, *Sov. J. Nucl. Phys.* **2**, 430 (1966); S.D. Drell and A.C. Hearn, *Phys. Rev. Lett.* **16**, 908 (1966).

12. K. Helbing, Proc. GDH2004, Norfolk 1–5 June, 2004, in preparation.
13. B. Lannoy, Ph.D. thesis, University of Gent, 2000.
14. M. McCormick et al., *Phys. Rev.* **C53** (1996) 41.
15. D. Drechsel, et al., *Nucl. Phys.* **A645** (1999) 145.
16. H. Olsen, L.C. Maximon, *Phys. Rev.* **114** (1959) 887.
17. T. Rostomyan, Ph.D. thesis in prep., University of Gent.
18. C.A. Rovelli, Diploma thesis, University of Pavia, 2003.
19. M. Schwamb, H. Arenhövel, *Nucl. Phys.* **A696** (2001) 556–580.
20. M. Schwamb, H. Arenhövel, *Nucl. Phys.* **A690** (2001) 647.
21. M. Schwamb, H. Arenhövel, *Nucl. Phys.* **A690** (2001) 682.
22. M. Schwamb, private communication, 2003.